Influence of substrate temperature on the morphological, structural, optical and electrical properties of nanostructured CuO thin films synthesized by spray pyrolysis technique

P. DATTA[a,b], M. SHARMIN[c], J. PODDER[c,*], S. CHOUDHURY[a]
a Department of Physics, University of Dhaka, Dhaka-1000, Bangladesh
b Nuclear Power Plant Company Bangladesh Limited, Rooppur NPP Bhaban, Dhaka-1000, Bangladesh
c Department of Physics, Bangladesh University of Engineering and Technology, Dhaka-1000, Bangladesh

Nanostructured copper oxide (CuO) thin films have been synthesized onto the glass substrates from aqueous solutions of copper (II) acetate monohydrate precursor salt by a cost effective spray pyrolysis technique at various substrate temperatures between 473 and 673 K. The effects of varying substrate temperature on the structure, surface morphology, optical and electrical properties of the synthesized CuO thin films were studied. Scanning Electron Microscopic (SEM) images revealed agglomerated nanoparticles on the surface of CuO thin films. X-Ray Diffraction (XRD) analysis revealed monoclinic structure with the predominant ($\bar{1}$11) orientation of the synthesized films. Crystallite size increased (9.15 to 10.29 nm) with the increase of substrate temperature. In UV-vis-NIR spectroscopy, CuO thin films showed higher transparency in the NIR region. An optical band gap of CuO thin film was found in the range of 2.04 - 2.49 eV. Transmittance and band gap decreased with the increase of substrate temperature up to 573 K and found to increase at 673 K. On the other hand, extinction coefficient and refractive index increased with the increase of substrate temperature up to 573 K and decreased afterwards. Electrical resistivity of CuO thin films was found in the range 1.16 ×10³ - 4.61 ×10³ Ω-m and decreased with the increment of the substrate temperature up to 573 K. Activation energies of CuO thin film were found in the range 0.08 - 0.57 eV. Hence, we report the influence of substrate temperature for the synthesis of nanostructured CuO thin films, best fit for optoelectronic applications.

(Received June 3, 2020; accepted February 15, 2021)

Keywords: Spray pyrolysis, CuO, SEM, XRD, Band gap, Activation energy

1. Introduction

The development of p-type transition metal oxides is one of the key technologies for pn-junction-based devices, such as light-emitting diodes, transistors, etc. [1]. Cupric oxide (CuO) is one of the well-known p-type transition metal oxide materials with a narrow band gap (1.2–1.9 eV) [2-4]. CuO has received considerable attention in recent years due to its unique properties and wide application range in gas sensors [5], biosensors [6], solar cells [7], high T_c superconductors [8], lithium ion batteries [9], catalysts [10], etc. CuO has been an interesting material because of its low cost, non-toxicity, abundant availability and relatively simple formation of oxide [11]. Many efforts have been made to fabricate nanostructured CuO, including nanoparticles [10], nanorods [12], nanowires [13], nanoplates [14], and nanotubes [15], to enhance its performance. It is known that shape controlled morphologies highly affect the properties of the nanomaterials. Thin films of CuO has been deposited by several deposition techniques, including solution method [14], DC magnetron sputtering [16], sol-gel spin coating [17], successive ionic layer adsorption and reaction [18], spray pyrolysis [19], etc. Among various deposition techniques spray pyrolysis is a simple, very easy, cost effective and efficient technique for large area deposition of films with the nice microstructural control [20, 21]. In spray pyrolysis technique (SPT), various deposition parameters [22] play important role during the synthesis of film and hence they influence the quality, structure, morphology and overall properties of the film. Growth kinetics of the thin films in SPT is strongly dependent on temperature when pyrolysis occurs on the surface of the substrate [22]. It can be said that substrate temperature is the most significant deposition parameter in SPT. Many research groups are working on the optimization of various deposition parameters in SPT during synthesizing CuO thin films. Naveena et al. [19] studied the influence of various precursors of SPT prepared CuO thin films on their structural, optical, morphological and electrical properties. They found that copper (II) nitrate was the most sensible choice for obtaining an effective photo-absorber layer in CuO based solar cell. Moumen et al. [23] investigated the effect of CuCl₂ precursor concentration on the structural and optical properties for CuO thin films deposited by SPT. They reported that CuO thin films prepared from 0.1 M solution of CuCl₂ precursor had the better crystalline structure and lower band gap. Prabu et al.

[24] reported the effect of substrate temperature on the CuO thin films prepared by SPT using 0.04 M solution of copper (II) acetate monohydrate and glucose dissolved in distilled water and 2-propanol. They studied the structure and properties of CuO thin films in the substrate temperatures range of 250 - 320 °C (523 – 593 K) and reported the formation of mixed structure of Cu_2O and CuO at 310 and 320 °C (583 and593 K). It is noticed that not much research have been reported on the effect of substrate temperature of CuO thin films in a relatively longer range 473 – 673 K. The major objective of this work was to find out the optimum substrate temperature for achieving CuO thin films with better structure, surface morphology, optical and electrical properties. The deposition conditions other than substrate temperature were chosen different from those found in earlier reports [19, 23, 24].

2. Experimental

2.1. Deposition of CuO thin films

The working solution was prepared by dissolving copper (II) acetate monohydrate [$Cu(CH_3COO)_2.H_2O$] (purity 99%) precursor into distilled water. Molar concentration of spray solution was 0.10 M. CuO thin films were prepared onto microscope glass substrates. The substrates were cleaned ultrasonically with ethanol and distilled water. Substrate temperature was adjusted using a variac and measured by Copper-Constantan thermocouple. CuO thin films were prepared at different substrate temperatures ranging from 473 – 673 K. The distance between the spray nozzle and the substrate was maintained about 25 cm. The flow rate of the solution and compressor air pressure were adjusted to be about 1ml/min and 0.5 bar, respectively and both these deposition parameters were kept constant throughout the deposition. CuO films were deposited for 10 min.

2.2. Characterization of CuO thin films

Film thickness was measured using Fizeau fringe method [25]. A JEOL JSM-6490LA (Japan) analytical scanning electron microscope was used for recording the Scanning electron microscopic (SEM) images of CuO thin films at 10,000 magnifications. Chemical compositions of CuO was inspected using an electron dispersive spectrometer (JEOL EX-37001, Japan) associated with the SEM set up. X-Ray diffraction (XRD) analysis was done using an X'Pert PRO XRD Philips PW3040 (Netherlands) X-ray powder diffractometer in which X-rays of wavelength 1.54178 Å was used from CuK_α target and operated at input power of 60 kV and 55 mA. To study 2θ values, d-spacing value and full width at half maximum (FWHM) an "X'Pert Highscore" computer software was used. The optical properties of CuO thin films were studied using an OPTIZEN POP QX UV/Vis (Republic of Korea) dual beam UV-visible spectrophotometer in the wavelength range of 200-1100 nm at room temperature.

The electrical resistivity and sheet resistance of the thin films was investigated at room temperature (300 K) using a four-point probe set up. Temperature dependence of electrical conductivity of the films was studied in the range 303 - 423 K using four point probe method.

3. Results and discussion

3.1. Surface morphology analysis

The surface morphologies of CuO thin films deposited at the substrate temperatures 473, 523, 573 and 673 K are shown in Fig.1. The SEM images reveal that sprayed particles are adsorbed on to the glass substrates into clusters as the primary stage of nucleation. In Fig. 1, nanoparticles are observed on the surface of CuO thin films. CuO thin film deposited at 473 K consists of cracks and inhomogeneous distribution of agglomerated nanoparticles. It may be attributed to the incomplete reactions during deposition. Cracks are not found on the surfaces of the films deposited at the temperatures 523, 573 and 673 K. It indicates that at substrate temperatures higher than 523 K, reactions evenly occur on the substrate surface under current deposition conditions. CuO films prepared at 523 and 573 K have regular size distribution of nanoparticle agglomerates and dense surface. There is no clearly visible agglomerates on the surface of CuO film prepared at 673 K, but there are some unevenly distributed pores on the surface. This featureless morphology at 673 K may occur because of the decompositions of the agglomerates due to high temperature effect. Formation of nanoparticle agglomerates in CuO thin films is also found in an earlier paper on SPT deposited CuO applying slightly different deposition parameters [24, 26].
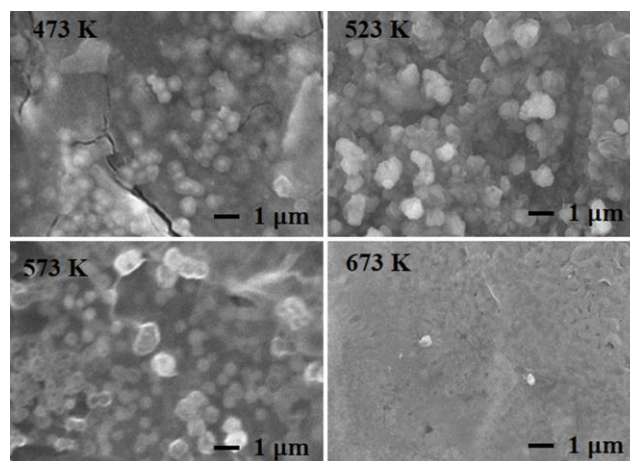
Fig. 1. SEM images of CuO thin films deposited at various substrate temperatures

3.2. Compositional analysis

Fig. 2 depicts the energy dispersive X-ray (EDX) spectrum of CuO thin film prepared at the substrate temperature 523 K. Peaks corresponding to Cu and O are found in the EDX spectra of the CuO thin films deposited

at various substrate temperatures; which approve the elemental compositions of the films. Quantitative analysis of CuO thin films shows that the films are stoichiometric. From the EDX analysis, the quantity of Cu and O are 58.65 and 41.35 at% in the CuO film prepared at the substrate temperature of 523 K. The amount of Cu and O are almost similar in the CuO films prepared at 473 and 573 K. The amount of O is higher in the film prepared at 673 K which may cause of the unevenly distributed pores on the surface of the film as found in the SEM image in Fig. 1.
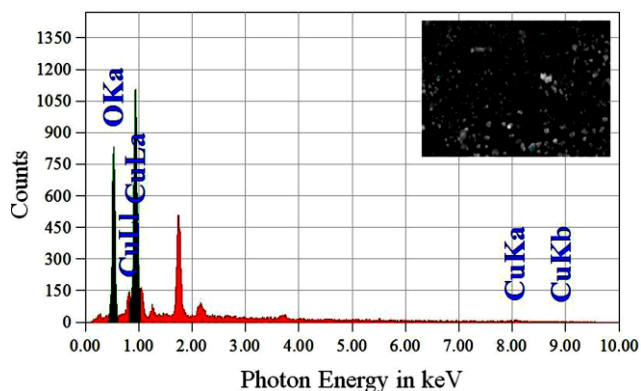
Fig. 2. EDX spectrum of CuO thin films deposited at 523 K substrate temperatures (color online)

3.3. Structural analysis

XRD patterns of CuO thin films synthesized at various substrate temperatures are shown in Fig. 3.
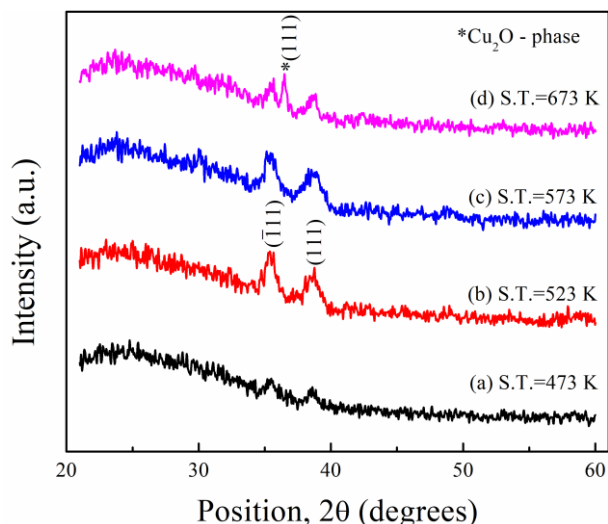
Fig. 3. The XRD pattern of CuO thin films deposited at different substrate temperatures (S. T.) (color online)

The XRD patterns are compared with the standard JCPDS data card no. 01-073-6023 [27]. CuO films have monoclinic crystalline structure with the existence of ($\bar{1}$11) and (111) planes. Similar XRD patterns are found for CuO thin films in some earlier papers [19, 23]. CuO thin film prepared at 473 K is less crystalline compared to others as

found in the XRD pattern in Fig. 3a. The intensity of ($\bar{1}$11) and (111) peaks increase with substrate temperature up to 573 K, which specifies betterment in crystallinity (Fig. 3b - 3c). The improvement in crystallinity may have occurred as a result of gaining adequate energy by the crystallites to orient in proper equilibrium sites at relatively higher substrate temperature [28]. In Fig. 3d, an additional peak is found near the ($\bar{1}$11) peak in the XRD pattern of CuO thin film prepared at 673 K. This additional peak is confirmed as the (111) peak related to Cu_2O (cubic) phase when compared with the JCPDS card no. 05-0667. In a transition metal oxide this is quite likely to form multiple oxidation states having different crystal structure in a same compound. It is found in the SEM image (Fig. 1) that the surface morphology is changed at 673 K substrate temperature which may be a direct consequence of formation of Cu_2O-CuO mixed phase in the film. Formation of Cu_2O-CuO mixed phase is also reported in another paper [24].

Table 1 represents various structural parameters calculated from the ($\bar{1}$11) peak data of CuO thin films. The peak position (2θ) is slightly shifted towards the lower angle and d-spacing is decreased upon the increase of substrate temperature up to 573 K. This may be related to the reorientation of crystallites with the increase of substrate temperature. A slight increase in 2θ and d-spacing is observed in the XRD pattern of CuO film prepared at 673 K which may be due to the appearance of additional Cu_2O-phase. When cubic Cu_2O-phase forms within the monoclinic CuO-phase, crystalline orientation along the predominant ($\bar{1}$11) plane is hampered. This may create lattice distortion and caused subsequent increase in 2θ and d-spacing.

Table 1. Structural parameters corresponding to ($\bar{1}$11) peak of CuO thin films

Sub. temp. (K)	2θ (deg)	d-spacing (Å)	D (nm)	ε × 10⁻³	δ × 10⁻³ (nm)⁻²
473	35.45	2.530	9.15	3.24	11.94
523	35.38	2.532	9.23	3.21	11.74
573	35.35	2.535	9.54	3.11	10.98
673	35.42	2.547	10.29	2.89	9.44

Crystallite Size (D) was calculated using Scherrer formula [29] in equation (1).

$$D = \frac{k\lambda}{\beta \cos\theta} \qquad (1)$$

In equation (1), k is shape factor which is a constant with the value 0.94, λ is the wavelength of X-rays, β is the FWHM and θ is the Bragg angle. The formula for determination of microstrain (ε) [30] is shown in the equation (2).

$$\varepsilon = \frac{\beta \cos \theta}{4} \qquad (2)$$

The dislocation density (δ) was evaluated using the Williamson and Smallman's formula [31],

$$\delta = \frac{1}{D^2} \qquad (3)$$

It is observed in Table 1 that D slightly increases with substrate temperature. It indicates that smaller crystallites form relatively larger agglomerated crystallites at relatively higher substrate temperature [26]. In some other papers, D is found in the range 8 - 33 nm [19, 23, 24, 32] which is in agreement with D in this work. ε and δ decrease with the rise of substrate temperature indicating the formation of less strained crystallites and reduction of dislocations along the preferred direction with the change of crystalline phase at higher substrate temperature.

3.4. Optical characterization

Optical transmittance (T%) spectra of CuO thin films deposited at various substrate temperatures are displayed in Fig. 4. CuO films are transparent in the near infrared (NIR) region. The maximum T% is found for CuO film prepared at 473 K and the value is about 86%. Usually CuO thin films are not so highly transparent and it is found to be much less than 80% in some published papers [23, 24, 32]. Since, there are significantly visible cracks in the SEM image of CuO film prepared at 473 K (Fig. 1), the film has such a high transparency.
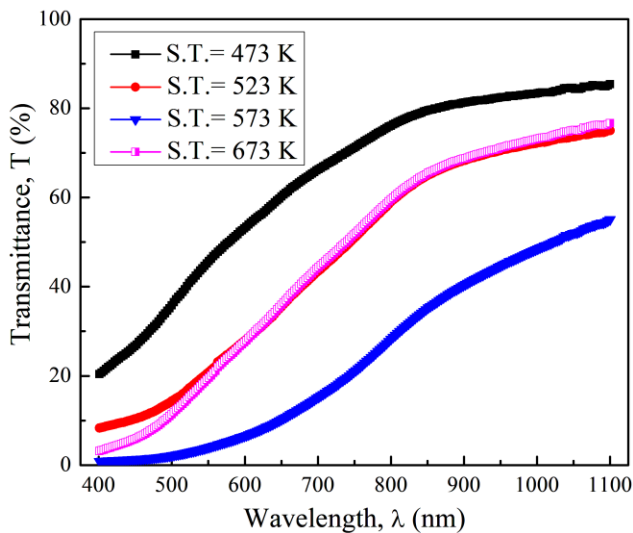
Fig. 4. Transmittance spectra for CuO thin films deposited at various substrate temperatures (color online)

T% of CuO thin films drops with substrate temperature up to 573 K which may be cause of the removal of cracks and presence of closely spaced agglomerated nanoparticles in the films (Fig. 1). T% increases for the CuO thin film prepared at 673 K because

of the existence of unevenly distributed pores on the surface of the film which forms as a result of gaseous phase reaction of the spray droplets (Fig. 1). The maximum transparency region is shifted from visible towards the NIR upon the rise of substrate temperature. This red shift may cause of the thermal oxidation effect that tends to change the crystalline phase via changing the oxidation state of Cu [33].

Optical band gap (E_g) of CuO thin films evaluated using Tauc formula.

$$\alpha h\nu = B(h\nu - E_{opt})^{n'} \qquad (4)$$

In equation (4), $h\nu$ is the energy of absorbed photon, n' is the parameter connected with distribution of the density of states and *B* is a constant, called Tauc parameter and here $n' = \frac{1}{2}$ for allowed direct and $n'=2$ for allowed indirect transitions [34]. The Tauc plots of CuO thin films deposited at various substrate temperatures are shown in Fig. 5. E_g of CuO thin films were calculated from the extrapolation of the straight line portion of the Tauc plots and displayed in Table 2.
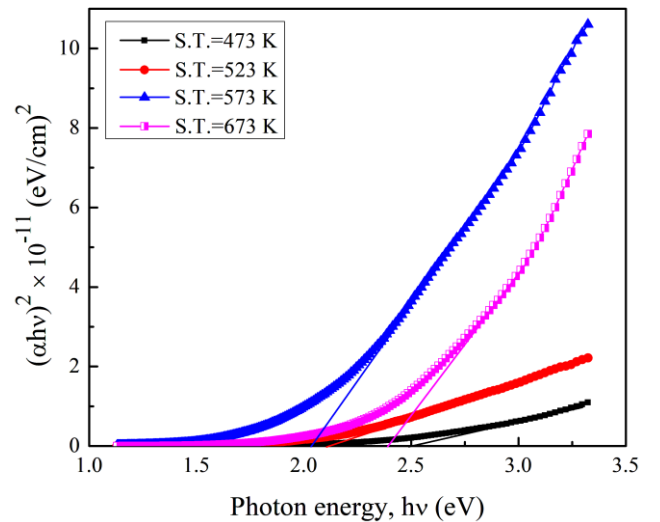
Fig. 5. Tauc plots of CuO thin films deposited at various substrate temperatures (color online)

E_g of CuO thin films decreases with substrate temperature up to 573 K. CuO prepared at 473 K has the largest band gap which may be because of less crystallinity. Since, CuO films prepared at 523 and 573 K have well defined monoclinic phase, E_g of those films matches nicely with the previously published E_g values of CuO ranging from 1.7 to 2.11 eV [18, 24]. E_g is found high for CuO film prepared at 673 K. This increment may happen due to the combined effect of transformation of crystalline phase from CuO to Cu_2O-CuO phase mixture in the film and uneven porous surface as seen in SEM image (Fig. 1). In an earlier paper it was written that T% depended on the film thickness which increased abruptly with substrate temperature [24]. Since, in our work film thickness values are nearly equal; thus the actual effect of

increase of substrate temperature on the structure and properties is observed here.

Table 2. Optical parameters CuO thin films deposited at various substrate temperatures

Sub. temp. (K)	$d \pm 8.2$ (nm)	E_g (eV)	k at 950 nm	n at 950 nm
473	181	2.49	0.08	1.86
523	182	2.11	0.14	2.20
573	162	2.04	0.38	2.58
673	148	2.40	0.17	2.18

Absorption coefficient (α) of CuO thin films was calculated from the absorbance (A) data using the following relation [35].

$$\alpha = \frac{2.303A}{d} \tag{5}$$

In equation (5), "*d*" is the film thickness whose values are shown in Table 2. Extinction coefficient (k) of CuO thin films was computed using α-values in the following equation.

$$k = \frac{\alpha\lambda}{4\pi} \tag{6}$$
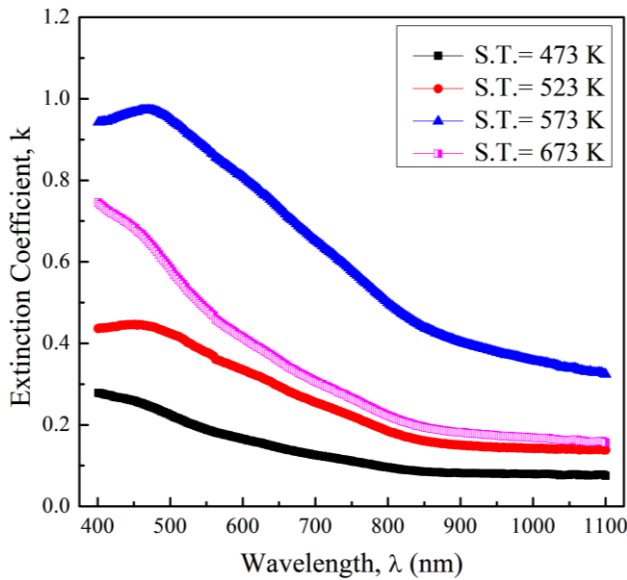
Fig. 6. Variation of extinction coefficient with wavelength for CuO thin films (color online)

The k-values of CuO are plotted against photon wavelength (λ) in Fig. 6. "k" is found to be varying in the range 0.07 and 0.97 which are in good agreement with the previously reported k-values of CuO thin films [23, 26]. The k-values at the wavelength 950 nm which is in the NIR region are shown in the Table 2. The CuO film deposited at 473 K has low k-value which indicates less amount of photon absorption in the film. The k-values rise

for the CuO films prepared at 523 and 573K, an indication of the increase of photon absorption in the films. CuO film deposited at 673 K shows low k-value due to the presence of unevenly distributed pores on the surface of the film and patternless morphology.
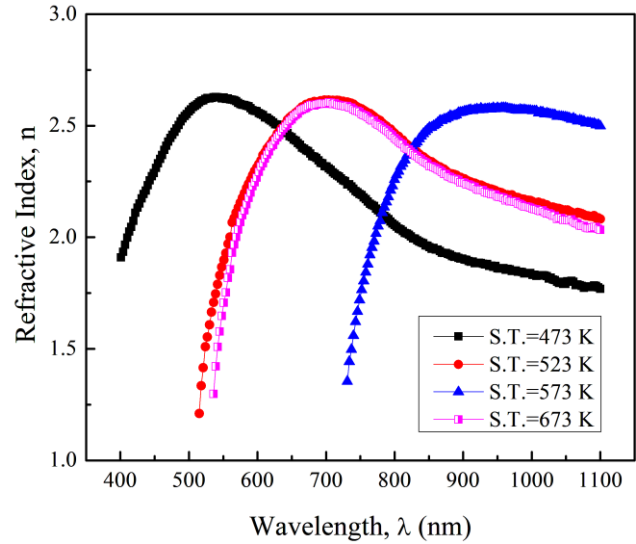
Fig. 7. Variation of refractive index with wavelength for CuO thin films (color online)

Refractive index (n) of CuO thin films was calculated using the equation (7) [36].

$$n = \left(\frac{1-R}{1+R}\right) + \sqrt{\left[\frac{4R}{(1-R)^2}\right] - k^2} \tag{7}$$

Here, R is the reflectance of the CuO films, calculated from the T% and A data.

In Fig. 6, n of CuO thin films is plotted against λ. Fig. 7 shows that n reaches the maxima, then slightly decreases and becomes constant. Similar pattern of variation of n with λ is found in some other papers on CuO thin films [23, 26]. It is observed that n changes between 1.21 and 2.63 which is also consistent with previously reported values [26]. In Table 2, n-values of CuO thin films at λ=950 nm are shown. The n-value at 950 nm increases with substrate temperature up to 573 K inferring the formation of CuO film with the increase of optical density. CuO film prepared at 673 K has less n-value and it can be said to have less optical density.

3.5. Electrical measurements

Electrical resistivity (ρ), conductivity (σ) and sheet resistance (R_s) of CuO thin films were calculated using the formulas in equations (8), (9) and (10), respectively.

$$\rho = 2\pi S \frac{V}{I} \tag{8}$$

$$\sigma = \frac{1}{\rho} \tag{9}$$

$$R_S = \frac{\rho}{d} \tag{10}$$

Here, V is the floating potential difference between the inner probes, I is the current through outer pair of probes, S is the distance between two adjacent probes.

Table 3. Electrical parameters CuO thin films deposited at various substrate temperatures

Sub. temp. (K)	ρ ($\times 10^3$ Ω-m)	σ ($\times 10^{-4}$ Ω^{-1}-m^{-1})	R_s ($\times 10^9$ $\Omega/\square$)	ΔE_1 (eV)	ΔE_2 (eV)
473	4.61	2.17	25.33	0.28	0.45
523	2.42	4.13	13.37	0.27	0.29
573	1.16	8.62	7.19	0.08	0.57
673	2.37	4.21	16.01	0.56	0.28

Table 3 shows ρ, σ and R_s of CuO thin films measured at 300 K temperature. Here, ρ, σ and R_s of CuO are found in the order of 10^3 Ω-m, 10^{-4} Ω^{-1}-m^{-1} and 10^9 $\Omega/\square$, respectively. These values are in nice match with those reported in some other papers [26, 37] and higher than that reported for Cd doped CuO [38]. ρ and R_s values decrease with substrate temperature up to 573 K and then increase for the CuO film deposited at 673 K. Increase of ρ and R_s occur due to the increase of oxygen absorption from air after a certain substrate temperature. Absorbed oxygen is the most substantial background defect in SPT that simply diffuse into the crystal lattice when the films are deposited at higher substrate temperature [39]. In this work the CuO thin film synthesized at 573 K is the most electrically conductive film.

The equation used for determination of activation energy [40] is as follows.

$$\sigma = \sigma_o \exp\left(-\frac{\Delta E}{2k_B T}\right) \tag{11}$$

Here, σ_o is the pre-exponential factor, ΔE_a is the activation energy, k_B is the Boltzmann constant and T is the temperature in K. Here, the factor 2 is multiplied with k_B for the two relative processes representing ionization and hoping process caused by thermal activation.

The Arrhenius plot indicates the thermally activated conduction [41]. The σ-values of CuO thin film are determined in the temperature range of 303 - 423 K. In Fig. 8, $ln\sigma$ is plotted against 1000/T. Fig. 8 indicates the increase of σ with the rise of T confirming the semiconducting nature of the CuO films. Each $ln\sigma$ vs 1000/T plot in Fig. 8 consists of two regions of conduction mechanism. So, there are two ΔE_a-values for each CuO film. ΔE_1 and ΔE_2 are the activation energies in the

temperature ranges 303 - 363 K and 363 - 423 K, respectively. ΔE_a-values are found in the range 0.08 - 0.57 eV. In some earlier literatures, ΔE_a-values for copper oxide thin films were found in the range 0.012 to 0.56 eV [24, 42, 43]; in which the films were deposited under different deposition conditions or techniques. It can be said that deposition conditions highly affect ΔE_a-values of copper oxide.
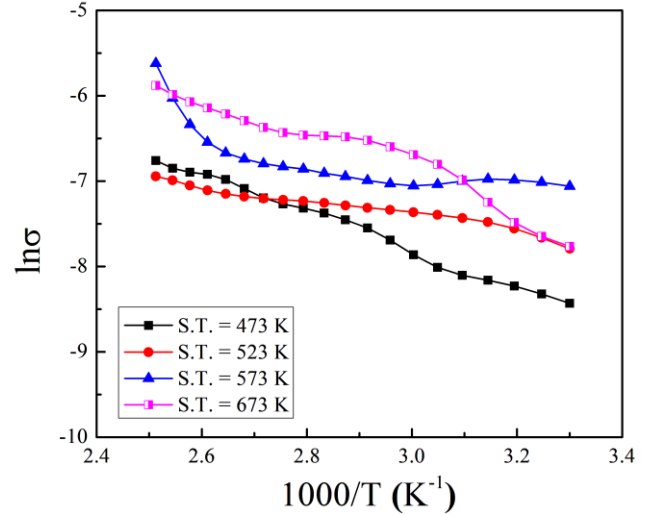
Fig. 8. The $ln\sigma$ vs 1000/T plots of CuO thin films prepared at various substrate temperatures (color online)

In Table 3, ΔE_1 falls with the increase of substrate temperature up to 573 K. It indicates the requirement of less energy for carrier hopping mechanism in the film in the temperature range 303 - 363 K. On the other hand, CuO film prepared at 673 K has a very high ΔE_1. It can be said that the carrier transport faces difficulty due to the presence of Cu$_2$O-CuO mixed phase or the larger amount of adsorbed oxygen in the film (as observed from the XRD spectra). ΔE_2 is found to the larger than ΔE_1 for each CuO film deposited between 473 and 573 K. This may happen because of the lessening of carrier generation sites at the oxygen vacancies and development of larger number of difficulties to inter-grain transport [44]. The difference between ΔE_1 and ΔE_2 of CuO thin film deposited at 523 K is 0.02, indicating stability in conduction behavior of the film. ΔE_2 of CuO film prepared at 673 K is reduced which may be due to the participation of carriers from the adsorbed oxygen sites at high temperature.

4. Conclusions

CuO thin films were successfully deposited onto the glass substrates at the substrate temperatures 473, 523, 573 and 673 K by SPT. SEM images of CuO thin films show that the film deposited at 523 and 573 K substrate temperatures have better surface morphology containing uniform distribution of nanoparticle agglomerates. XRD analysis revealed that CuO films having pure monoclinic crystalline phase are found for the films prepared at 523 and 573 K. The film prepared at 673 K has mixed Cu$_2$O-CuO crystalline phases. Crystallite sizes of the CuO

nanoparticles are found in the range 9.15 to 10.29 nm. E_g of CuO thin films deposited at 523 and 573 K are found to be 2.11 and 2.04, respectively. CuO thin film prepared at 573 K has the least electrical resistivity of 1.16×10^3 Ω-m and the lowest activation energy of 0.08 eV in the temperature range 303 - 363 K. Although CuO film prepared at 523 K has a higher electrical resistivity than that of the film deposited at 573 K, it shows a stable conduction mechanism with temperature. CuO thin film with better surface morphology, crystalline structure, narrowed band gap, high refractive index, low electrical resistivity and good conduction behavior is possible to fabricate at the substrate temperature 523 K and could be a suitable candidate for applications as near-infrared filters, sensors, catalysis, and semiconductors, etc.

References

[1] A. N. Banerjee, S. Kundoo, K. K Chattopadhyay, Thin Solid Films **440**(13), 5 (2003).

[2] I. Singh, R. K. Bedi, Appl. Surf. Sci. **257**(17), 7592 (2011).

[3] R. Sahay, J. Sundaramurthy, P. S. Kumar, V. Thavasi, S. G. Mhaisalkar, S. Ramakrishna, J. Solid State Chem. **186**, 261 (2012).

[4] L. Zheng, X. Liu, Mater. Lett. **61**(11-12), 2222 (2007).

[5] R. Li, J. Du, Y. Luan, Y. Xue, H. Zou, G. Zhuang, Z. Li, Sensors Actuat. B **168**, 156 (2012).

[6] K. Jindal, M. Tomar, V. Gupta, Biosens. Bioelectron. **38**(1), 11 (2012).

[7] H. Chang, M. Kao, K. Cho, S. Chen, K. Chu, C. Chen, Curr. Appl. Phys. **11**(4), 19 (2011).

[8] T. Jarlborg, Physica C **454**(1-2), 5 (2007).

[9] Z. Yin, Y. Ding, Q. Zheng, L. Guan, Electrochem. Commun. **20**, 40 (2012).

[10] S. M. Inamdar, V. K. More, S. K. Mandal, Tetrahedron Lett. **54**(6), 579 (2013).

[11] V. Figueiredo, E. Elangovan, G. Goncalves, P. Barquinha, L. Periera, N. Franco, E. Alves, R. Martins, E. Fortunato, Appl. Surf. Sci. **254**(13), 3949 (2008).

[12] Z. Yang, D. Wang, F. Li, D. Liu, P. Wang, X. Li, H. Yue, S. Peng, D. He, Mater. Lett. **90**, 4 (2013).

[13] W. Gao, S. Yang, S. Yang, L. Lv, Y. Du, Phys. Lett. A **375**(2), 180 (2010).

[14] F. Bayansal, S. Kahraman, G. Cankaya, H. A. Cetinkara, H. S. Gŭder, H. M. Cakmak, J. Alloys Compd. **509**(5), 2094 (2011).

[15] Y. Sun, L. Ma, B. Zhou, P. Gao, Int. J. Hydrog. Energy **37**(3), 2336 (2012).

[16] M. R. A. Cruz, D. Sanchez-Martinez, L. M. Torres-Martínez, Mater. Res. Bull. **122**, 110678 (2020).

[17] Y. Lim, C. S. Chua, C. J. J. Lee, D. Chi, Phys. Chem. Chem. Phys. **16**, 25928 (2014).

[18] O. Daoudi, Y. Qachaou, A. Raidou, K. Nouneh, M. Lharch M. Fahoume, Superlattices Microst. **127**, 93 (2019).

[19] D. Naveena, T. Logu, R. Dhanabal, K. Sethuraman, A. C. Bose, J. Mater. Sci. Mater. Electron. **30**(1), 561 (2019).

[20] D. Perednis, L. J. Gauckler, J. Electroceram. **14**(2), 103 (2005).

[21] P. S. Patil, Mater. Chem. Phys. **59**(3), 185 (1999).

[22] M. Sharmin, A.H. Bhuiyan, Appl. Phys. A **124**(1), 57 (2018).

[23] A. Moumen, B. Hartiti, P. Thevenin, M. Siadat, Opt. Quant. Electron. **49**(2), 70 (2017).

[24] R. D. Prabu, S. Valanarasu, V. Ganesh, M. Shkir, S. Al-Faify, A. Kathalingam, S. R. Srikumar, R. Chandramohan, Mater. Sci. Semicon. Proc. **74**, 129 (2018).

[25] S. Tolansky, Multiple Beam Interferometry of Surfaces and Films, Oxford Clarendon Press, London, 1948.

[26] M. Nesa, M. Sharmin, K. S. Hossain, A. H. Bhuiyan, J. Mater. Sci. Mater. Electron. **28**(17), 12523 (2017).

[27] S. Asbrink, L. J. Norrby, Acta Crystallogr. B **26**, 8 (1970).

[28] F. C. Akkari, M. Kanzaria, B. Rezig, Eur. Phys. J. Appl. Phys. **40**(1), 49 (2007).

[29] P. Scherrer, N. G. W. Goettingen, Math-Phys. Kl **1918**, 98 (1918).

[30] Y. Zhao, J. Zhang, J. Appl. Cryst. **41**(6), 1095 (2008).

[31] G. K. Williamson, R. E. Smallman, Philos. Mag. **1**(1), 34 (1956).

[32] M. G. Faraj, A. K. Kaka, H. D. Omar, ARO-The Scientific Journal of Koya University **7**(2), 10558 (2019).

[33] M. A. Rafea, N. Roushdy, J. Phys. D: Appl. Phys. **42**, 015413 (2009).

[34] E. A. Davies, N. F. Mott, Philos. Mag. **22**(179), 903 (1970).

[35] R. E. Hummel, Electronic Properties of Materials, 3rd Edition, Springer-Verlag, New York (2000).

[36] W. D. Callister Jr., Fundamentals of Materials Science and Engineering, John Wiley & Sons, New York (2001).

[37] M. L. Zeggar, M. S. Aida, N. Attaf, J. New Technol. Mater. **4**, 86 (2014).

[38] M. H. Babu, J. Podder, B. C. Dev, M. Sharmin, Surfaces and Interfaces **19**, 100459 (2020).

[39] M. Oztas, M. Bedir, Thin Solid Films **516**(8), 1703 (2008).

[40] L. L. Kazmerski, Polycrystalline and Amorphous
     Thin Films and Devices, Academic Press, New York
     (1980).

[41] M. M. Rahaman, K. M. A. Hussain, M. Sharmin,
     C. Das, S. Choudhury, Eur. Sci. J. **12**(27),
     7881 (2016).

[42] V. Dhanasekaran, T. Mahalingam, J. Nanosci.
     Nanotechnol. **13**(1), 250 (2013).

[43] A. Parretta, M. K. Jayaraj, A. D. Nocera, S. Loreti,
     L. Quercia, A. Agati, Phys. Stat. Sol. A **155**(2),
     399 (1996).

[44] E. Miller, D. Paluselli, B. Marsen, R. Rocheleau, Thin
     Solid Films **466**(1-2), 307 (2004).

_____
*Corresponding author: jpodder59@gmail.com